Differences between Physical Water Models and Steel Continuous Casters: A Theoretical Evaluation

R. Chaudhary, B. T. Rietow, B. G. Thomas
Department of Mechanical Science & Engineering,
University of Illinois at Urbana-Champaign,
1206 W Green Street, Urbana, IL, 61801, US

Abstract

Nonoptimal fluid flow patterns in the mold cause level fluctuations and excessive surface velocities at the top surface, which shears off and emulsifies liquid slag, leading to inclusions and other defects in the steel product. Physical water models are often used to investigate these phenomena. However of the solidifying shell, and the top-surface slag layer leads to significant differences in the flow behavior, relative to the real steel caster. Trying to include these effects presents other difficulties. Constructing smaller, scaled-down water models introduce further differences. These differences are investigated using computational models of both the water models and real casters. The Froude similarity criterion reasonably reproduces overall flow features for different scale models, so long as the flow regime stays fully turbulent. Flow in small scale water models behaves differently, if the flow regime becomes laminar. Neglecting the surface slag layer causes excessive surface velocities in a water model. Neglecting the solidifying shell causes unrealistic lower surface velocities and surface waves in the water model, especially for thinner cross sections. Thus, water models of thin slab casters may become unreliable.

Keywords: asymmetric flows, turbulence, casting speed, water models, scaling

1. Introduction

Optimization of fluid flow in continuous casting can greatly impact this high-tonnage, energy intensive process, by improving quality at negligible cost. The process parameters which control the transient flow structures in a given mold shape include the nozzle type (slide gate or stopper rod, bifurcated or trifurcated etc.), port shape, port angle, SEN depth, casting speed, argon gas injection, and electromagnetic control. Plant measurements are extremely difficult at high temperatures and adverse environmental conditions in real casters, and constructing computational models that can accurately predict the subtle transient events which often control defect formation is difficult and computationally-intensive. Thus, physical modeling with scaled water models has been the favorite choice to understand and optimize the complex flow patterns in the mold [1-15], owing to the similar kinematic viscosity of water and steel, and the ease of constructing and visualizing flow in water models. What is the best way to construct and operate a water model and how accurately can it match flow behavior in the real caster? These are the questions addressed in this work.

2. Previous Work with Water Models

Szekely et al performed water model studies on radial and straight flow nozzles and recommended use of radial flow nozzles for inclusion removal [1]. Thomas *et. al.* produced a full-scale water model to simulate flow through a continuous thin-slab stainless steel caster [2]. Model predictions were found matching qualitatively with dye-injected flow patterns. Gupta *et. al.* developed water models to investigate the asymmetry and transient oscillations of fluid flow inside the mold [3]. Through additional work, Gupta performed a parametric study to investigate flow asymmetries in the mold, varying the mold dimensions, casting speed, nozzle submersion and nozzle type [4]. It was concluded that the fixed bottom wall of his water model appeared to affect flow in the lower mold region by suppressing the asymmetries. Honeyands and Herberton [5] observed surface level fluctuations in a thin-slab water model with a characteristic frequency that increased with casting speed. Lawson and Davidson [6] used Laser Doppler Velocimetry (LDV) to measure oscillatory flow in a 0.33-scale thin-slab water model. Low frequency oscillation modes had the most oscillatory energy, especially below 5Hz in the jets, and below 0.2Hz in the mold overall. This is consistent with findings of Sivaramakrishnan et al [7] from velocities measured in a 0.4-scale water model using Particle Image Velocimetry (PIV). Yuan et al [8] performed Large Eddy Simulation (LES) and experimental studies on 0.4-scale water model. LES matched experiments reasonably and complex time evolving turbulent flow structures were reported in the mold. Theodorakakos et al [9] studied steel-slag interface through numerical and experimental work on a water model. A critical casting speed was proposed leading to interface instability and emulsification. Ramos-banderas et al [10] matched LES predictions with digital particle image velocimetry (DPIV) measurements on a water model. Periodic behavior of instantaneous velocities caused velocity spikes in the steady operation of the mold. Li et al [11] created a snake shaped Plexiglas water model to study vortexing flow in the mold and vortex flow was reported as the direct consequence of three-dimensional biased flow in the mold. Zhang et al [12] investigated fluid flow in the mold region of a continuous slab caster with 0.6 scale (based upon Froude & weber number similarity) water model, plant measurements and numerical simulations. Gupta and Lahiri [13] carried out experimental studies to model the effect of slag-steel interface and proposed viscosity and density ratios of slag to steel should be equal to that of top-fluid or beads to water to model slag-steel interface properly. Chaudhary et al [14] performed numerical and experimental studies on a $1/3^{rd}$ water model of a steel caster. Based upon combined numerical and experimental understanding, conclusions were extended for steel caster.

Although, so far, a large number of numerical and experimental studies have been performed using water models to understand the complex time varying turbulent flow structures in the continuous casting molds, but none of them truly focused on the limitations and smartness of water modeling in replicating time varying velocities and free surface waves in the caster and thus remains a topic of current interest.

3. Water Model Construction and Operation Criteria

To ensure that the water modeling of a continuous casting captures the flow features of a real casting process, it is important to overcome the major differences between them:

1. Water and steel have greatly different properties, such as density and viscosity and surface tension.

2. Water models often are constructed at reduced scale, to lower cost.
3. Water models lack shell solidification even though sometimes tapered walls on wide and narrow faces are manufactured to match solidification front but still they lack in mass and momentum extraction caused by real solidification. Also in addition to mass and momentum sink terms the vertical wide and narrow faces should move downward with casting speed.
4. In water models, top surface is usually opened to atmosphere however in steel casters it is covered with slag whose viscosity is highly sensitive to temperature.
5. Water model at the bottom usually delivers water to a tank to be pumped back into the tundish for recirculation. In real casters, steel liquid domain tapers due to shell and steel ends up being completely solid at the bottom.
6. Since, real casters have continuous solidification of steel and temperature varies significantly within mold therefore buoyancy effects can be significant which are usually not modeled in water models.

To address these differences, scaling criteria have been developed. Kinematic viscosity matches at ~27^{o}C and is around 15% higher in water at ~20^{o}C. Thus, for single-phase flow, water and steel behave very similarly. Their surface tensions greatly differ. To balance inertial and viscous forces, theoretically requires Reynolds similarity, meaning that the water model should have the same Reynolds number ($\mathrm{Re} = D_h V_{casting} / \nu$) as the caster.

1. Because the free surface-flow is also important, the Froude number, which balances inertia and gravity, ($Fr = V_{casting} / \sqrt{g h_{mold}}$) should be matched as well.
2. To match both Reynolds and Froude similarity simultaneously needs a full-scale water model, assuming that the kinematic viscosities of steel and water are roughly equal. However, once the flow is fully turbulent, the effect of Reynolds number is small, so the requirement of satisfying Reynolds similarity is often relaxed, and a small-scale model can often be used [13]. In this case, the flow rate must be decreased in the water model as follows: $\lambda^{2.5}$. This means that the casting speed must be dropped by a factor of $\lambda^{0.5}$, or 0.6 for a 1/3 scale model (λ=1/3, geometric scaling factor)
3. To balance inertia and surface tension also requires satisfying Weber similarity.

To satisfy Weber and Froude similarities together requires a 0.6-scale model [12]. However, the phenomena involving surface tension are very complex, and usually involve slag-steel interaction, multiphase flow, and other important phenomena such as bubble size, slag/steel viscosities, slag and steel density, droplet emulsification which cannot properly incorporated with a simple water model. Thus, it is likely not helpful to match Weber number without matching many other phenomena as well, which is extremely difficult to achieve.

Of these main differences, shell solidification and top free surface effects are most important especially in the upper region of the mold. Since model domains can always be extended at the bottom therefore bottom effects are not that important in the upper region.

A mathematical modeling approach has been used to study the effect of free-surface and shell-solidification through mass and momentum sink in 1/3rd and full scale water models of thick-slab steel caster and full-scale water model of thin-slab funnel mold and following effects have been analyzed:

- Effect of scaling (full and 1/3), top-surface layer treatment, (air, oil, or beads) shell solidification, relative slab thickness (thick and thin caster).

- Effect on flow pattern, especially impingement point, surface velocity, and surface level fluctuations.
- The results from different cases are compared to determine the accuracy of different types of water models, and to suggest guidelines for water model construction and operation.

4. Computational Model Investigation of Water Model Accuracy

A 3-d computational model with Reynolds Averaged Navier-Stokes (RANS) approach to model turbulent flow in the nozzle and mold of water models and casters was formulated. Closure for Reynolds stresses was achieved with standard k-ε turbulence model to model turbulence in terms of eddy viscosity. Wall functions were used at the wall boundaries which allowed coarser mesh close to the walls compared to Large Eddy Simulation (LES) and Direct Numerical Simulation (DNS). To model the effect of shell solidification in the casters, flow domain was modified according to shell growth and mass and momentum sink terms were added as per the formulations given elsewhere [14]. Formulated computational model was validated by comparing model predictions in the mold with time-averaged PIV, impeller velocity and turbulence measurements [14]. More details on model formulation and validation are given elsewhere [14].

First, thick-slab mold and thin-slab funnel mold simulations were created. The domains in two were modified to incorporate the solidification front into the liquid pool dimensions (via CON1D [15] shell thickness predictions, smoothed to neglect the effect of oscillation marks and surface irregularities). Therefore, a slightly different domain with curved sides and a sloping inner liquid cavity was used for the steel case. Fig-1(c) gives the shell thickness below meniscus in both thick-slab caster and thin-slab funnel mold. The effects of solidification were implemented through the placement of thin mass/momentum sink elements at the shell front. The shell interface was moved with casting speed in the casting direction. Top surface was assumed flat and no-slip boundary condition was applied to closely model the effect of high viscosity slag on the free surface. Dimensional and parametric details along with fluid properties on steel caster models are given in Table-1. Fig-1 (a) shows the schematic of modeled think-slab caster with dimensions with shell shown in red dotted lines and corresponding full scale water model without shell. Fig. 1(b) gives dimensional details about the bottom-well of the SEN. Fig. 2 gives the dimensional details on thin-slab funnel mold.

Corresponding to above mentioned casters, full scale (thin-slab funnel-mold), full-scale and 1/3rd scale (thick-slab mold) water model simulations were also created. The domain for the water model simulation simply consists of the unmodified mold dimensions and the exiting slab dimensions without any mass/momentum removal. In full-scale water model of the funnel mold, vertical wide and narrow faces were moved towards bottom with casting speed and purely the effect of shell solidification implemented through mass/momentum sink terms was analyzed. At top surface both no-slip and free-slip boundary conditions have been implemented to simulate the effect of air, high viscosity oil [13]) and beads ($\rho_{beads} = \rho_{water}\rho_{slag} / \rho_{steel}$). Dimensional and parametric details along with fluid properties on water models are given in Table-1. Due to model complexities involved in free-surface flows, top surface was assumed fixed and flat, increase in pressure along this surface allows for an estimation of the free surface deformation

using energy conservation laws. The following equation has been employed to estimate free surface deformation along this top surface [16]:

$$\Delta Height = \left(p - p_o\right) / \left(g\left(\rho_{steel} - \rho_{slag}\right)\right) \qquad (1)$$

Table-2 shows the cases modeled and used to study the water modeling of steel caster. In thick-slab mold category, full-scale water model with flat and no-slip top surface (to model viscous oil and beads) and 1/3rd water model with flat and free-slip (to model air)/no-slip top surface (to model viscous oil and beads) for two Froude numbers (Fr=0.005 and 0.0152) along with caster at one Froude number (Fr=0.005) with mass and momentum sink terms have been analyzed (Case: 1-7). Furthermore, study has been extended in thin-slab funnel mold to see the effect of mold thickness on water modeling because of shell-solidification (Case: 8-9).

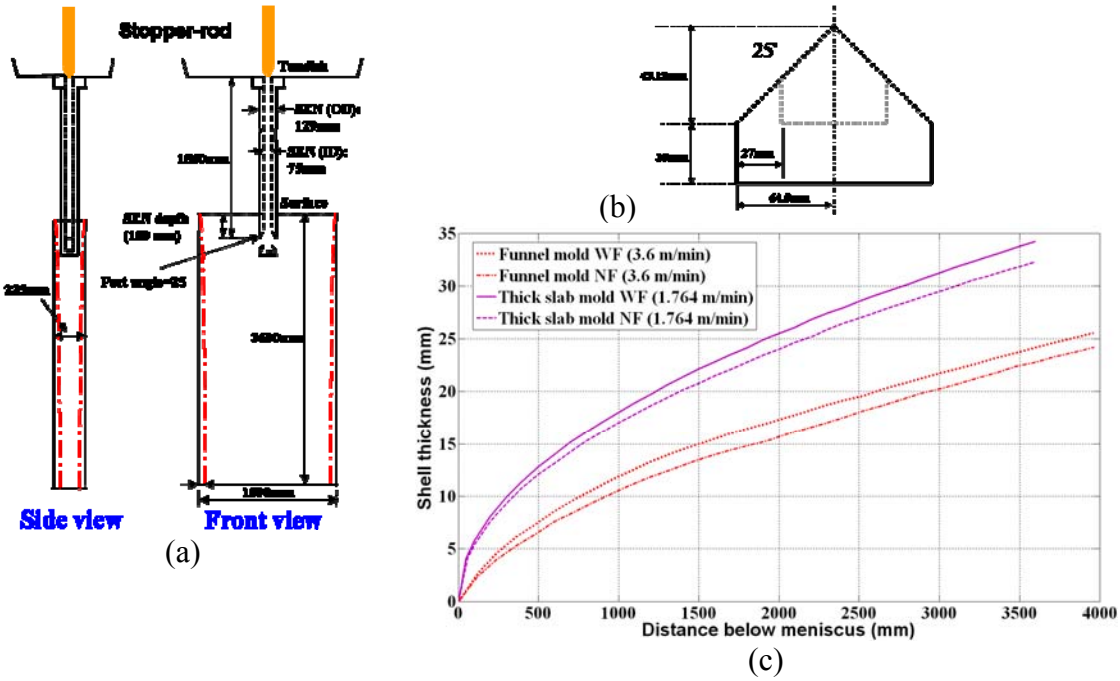

Fig-1 (a) Schamatic of thick-slab steel caster with shell and full-scale water model without shell (b) SEN bottom well (c) Shell thickness as a function of distance below meniscus for thick-slab mold as well as thin-slab funnel mold

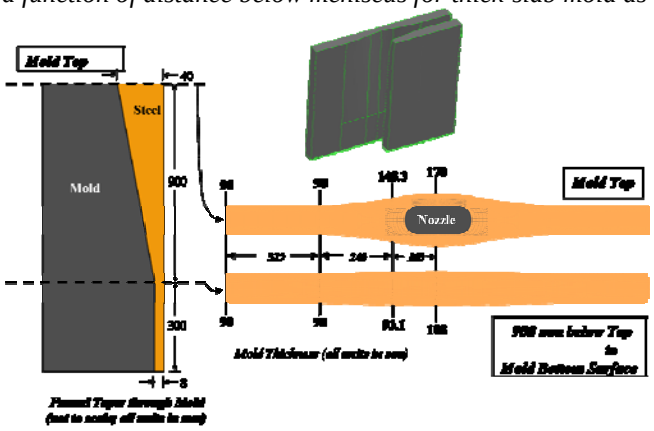

Fig-2 Dimensional details on thin-slab funnel mold model

Table-1 Dimensional details, process parameters and properties used for water models and casters

Parameter/property	Thick slab			Thin-slab funnel mold	
	Caster	Full-scale water model (@27°C)	1/3rd water model (@ 20 °C)	Funnel mold	Full-scale water model (@ 20 °C)
Casting speed (m/min)	1.764	1.764, 5.44	1.0186,3.145	3.6	3.6
Mold width (mm)	1500	1500	500	1450	1450
Mold thickness (mm)	225	225	75	90/170	90/170
Mold length (mm)	3600	3600	1200	1200	1200
SEN depth (mm)	180	180	60	265	265
Nozzle port (mm) (H,W,T)	80.1, 69.9	80.1, 69.9	26.7, 23.3	141,127, 28	141, 127, 28
Nozzle port angle (deg)	25	25	25	9.8(vertical)	9.8(vertical)
Nozzle bore ID/OD (mm)	75/129	75/129	25/43	80	80
Density (kg/m^3)	7020	1.0	998.2	7020	998.2
Dynamic viscosity (Ns/m^2)	0.006	0.00085	0.001	0.006	0.001
Kinematic viscosity (m^2/s)	$0.85x10^{-06}$	$0.85x10^{-06}$@27 °C	$1.0x10^{-06}$ @ 20 °C	$0.85x10^{-06}$	$1.0x10^{-06}$@20 °C
Fluid above top surface (density, kg/m^3))	Slag (ρ=3000)	Beads(ρ=426), oil (ρ=890)	Air(ρ=1.18),beads (ρ=426),oil(ρ=890)	Slag (ρ=3000)	Beads (ρ=426)
Mass/momentum sink with shell solidification	Yes	No	No	Yes	No
Domain modeled (nozzle & mold)	¼	¼	¼	½	½
Top surface condition	No-slip	No-slip	Free- and no-slip	No-slip	No-slip
Vertical downward motion of wide and narrow faces with casting speed	Yes	No	No	Yes	Yes

Table-2 Various water models and casters modeled

Thick-slab mold					
Case no	Type of model	Top surface condition	Froude no (Fr)	Reynolds no (Re)	Casting speed (m/min)
Case:1	Steel caster	No-slip (slag)	0.005	--	1.764
Case:2	Full-scale water model at 25 °C	No-slip (beads & oil)	0.005	13462	1.764
Case:3	Full-scale water model at 25 °C	No-slip (beads & oil)	0.0152	41519	5.44
Case:4	1/3rd water model at 20 °C	No-slip (beads & oil)	0.0152	6817	3.141
Case:5	1/3rd water model at 20 °C	Free-slip (air)	0.0152	6817	3.141
Case:6	1/3rd water model at 20 °C	No-slip (beads & oil)	0.005	2203	1.0186
Case:7	1/3rd water model at 20 °C	Free-slip (air)	0.005	2203	1.0186
Thin-slab funnel mold					
Case:8	Steel caster	No-slip (slag)	--	--	3.6
Case:9	Full-scale water model at 20 °C	No-slip (beads)	--	--	3.6

5. Results and Discussion

5.1. Effect of Scaling

Fig-3(a) and (b) shows the velocity contours and streamlines at mold-mid plane between wide faces at Fr=0.005 in 1/3rd and full-scale water models with no-slip condition at the top. Since only Froude similarity is satisfied and full-scale is 3 times in all linear dimensions, maximum velocity in full-scale is $\sqrt{3}$ times that in 1/3rd water model. Streamline patterns are quite consistent showing standard double roll pattern and are found matching nicely especially in the upper recirculation zone. Fig-4 quantifies scaled free-surface velocity magnitude in upper zone at 5mm below free surface in 1/3rd water model and 15 mm from free-surface in full-scale water

model & caster. As suggested in velocity contours, velocity magnitude matched nicely in-between 1/3rd and full-scale water models. In the lower region, flow patterns are quite different and the reason for this is the detachment of slower jet from narrow face in 1/3rd water model. At the same Froude number, in full-scale water model, jet has enough momentum and stays attached and thus causing difference. Reynolds number in 1/3rd water model suggest it being in transition regime while full-scale model in fully turbulent regime at same Fr=0.005. Fig-5 quantifies the mismatch in lower region through downward velocity and signifying the importance of difference of flow regimes in two.

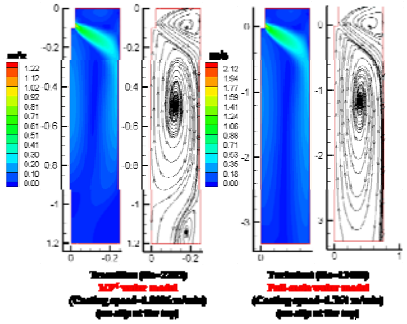

(a) *(b)*

Fig-3 Comparison of velocity contours and streamlines in (a) 1/3rd and (b) full-scale water model (with no-slip boundary condition on the top) (Fr=0.005)

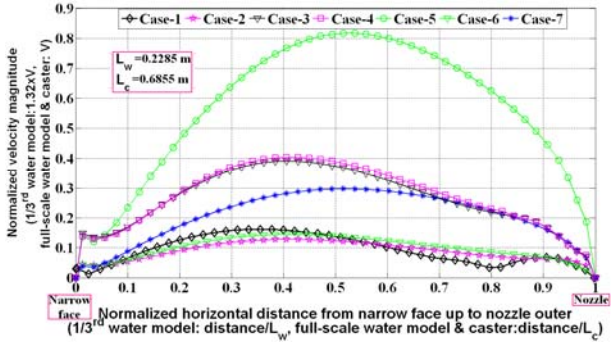

Fig-4 Scaled velocity magnitude plotted as a function of normalized distance from narrow face to SEN at mid-plane between wide faces at 5 mm from surface in 1/3rd and at 15mm from surface in full-scale water model & caster

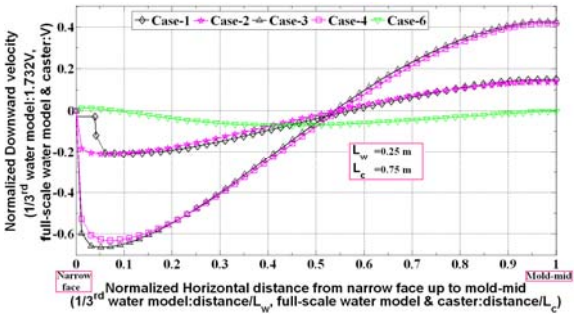

Fig-5 Scaled downward velocity plotted as a function of normalized distance from narrow face up to mold-mid at 1.0 m from surface in 1/3rd and 3.0 m from surface in full-scale water model & caster

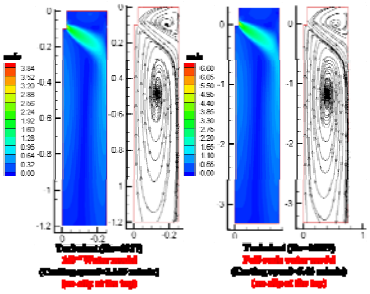

(a) *(b)*

Fig-6 Comparison of velocity contours and streamlines in (a) 1/3rd and (b) full-scale water model(with no-slip condition on the top) (Fr=0.0152)

To ascertain regime difference on non-matching of flow patterns, simulations were also created at a higher Froude number (Fr=0.0152, ensuring high enough Reynolds number (Re=6817) to keep 1/3rd water model in turbulent regime). Fig-6(a) and (b) shows the velocity contours and streamlines at higher Froude number (Fr=0.0152). 1/3rd and full-scale water models showed nice agreement in streamlines and flow patterns in the whole domain. Although such high casting speed (5.44 m/min) is practically difficult to achieve, but importance of flow regime is clearly expressed through this case. Fig-5 and 7 show scaled downward velocity at different vertical distances from mold surface. Downward velocity at both vertical locations is found matching nicely in-between 1/3rd and full scale water model at higher Froude number (Fr=0.0152). Fig-8 shows scaled horizontal velocity along a vertical line which is 50 mm from narrow face in 1/3rd water model and 150mm from narrow face in full-scale water model. Velocities matched nicely at both Froude numbers especially in the upper zone. Higher Froude number case gives stronger

jet and higher reverse velocity at the free surface. Fig-9 shows scaled free surface level. Higher Froude number showed higher surface wave and free surface level calculated assuming beads on the top at both Froude numbers (Fr=0.005 and Fr=0.0152) matched nicely in 1/3rd and full scale water models.

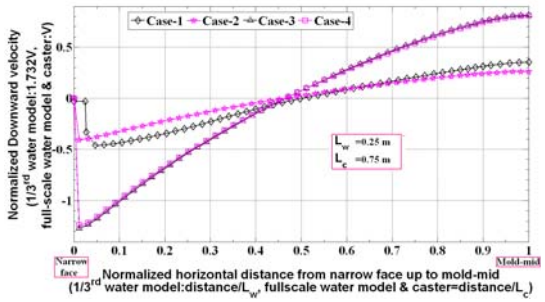

Fig-7 Scaled downward velocity plotted as a function of normalized distance from narrow face up to mold-mid at 0.4 m from surface in 1/3rd and 1.2 m from surface in full-scale water model and caster

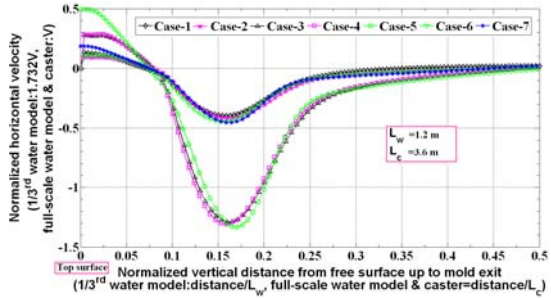

Fig-8 Scaled horizontal velocity as a function of normalized distance from free surface up to mold bottom in 1/3rd water model (at 50 mm from narrow face), full-scale water model and steel caster (at 150mm from narrow face)

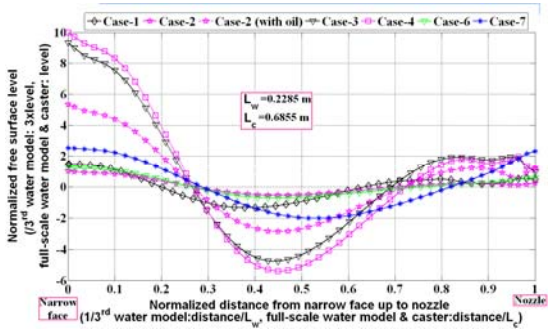

Fig-9 Scaled free surface level plotted as a function of normalized distance from narrow face up to nozzle in 1/3rd water model, full-scale water model and caster (Fr=0.005 & Fr=0.0152)

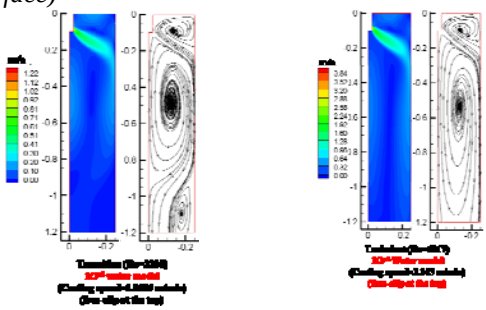

(a) *(b)*

Fig-10 Velocity contours and streamlines in 1/3rd water model (with free-slip- boundary condition on the top) (a) Fr=0.005 (b) Fr=0.0152

5.2. Effect of Slag

Fig-10 (a) and (b) shows velocity contours and streamlines at the mold-mid plane between wide faces in 1/3rd water model with free-slip condition at the top surface at Fr=0.005 and 0.0152 respectively. Higher velocity is seen in the upper region of the mold compared to no-slip cases at both Froude numbers. In Fig-4, surface velocity magnitude at 5 mm from surface in 1/3rd water model and 15 mm from surface in full-scale water model with free-slip is found ~2 times higher than in no-slip cases at both Froude numbers. Fig-8 shows the effect of the top boundary on the horizontal velocity in upper zone. Top surface boundary is found affecting velocity in upper zone up to 0.05 units normalized vertical distance afterwards around jet and in lower region effect disappears. Fig-9 shows scaled free surface level. Air on the top with free-slip boundary gives ~2 times surface wave than no-slip with beads on the top at both Froude Numbers (at Fr=0.0152, wave height is 20mm). Free-surface level with viscous oil is also plotted at Fr=0.005. Being heavier than beads and air (density: 890 vs 426 and 1.18 kg/m^3), oil with no-slip shows much higher amplitude surface wave compared to both free and no-slip cases with air and beads respectively. This finding is consistent with the experimental work of Gupta & Lahiri [14].

5.3. Effect of Shell and Mold Thickness

Fig-11 shows the velocity contour and streamlines at the mold mid-plane in steel caster at Fr=0.005. Maximum velocity is same as in full-scale water model since it is at the nozzle outlet. Flow patterns look qualitatively same (as in Fig-3 (b)) however quantitative differences are seen. In Fig-4, at Fr=0.005, caster with shell and no-slip at the top is found to be giving slightly higher scaled surface velocity close to narrow face and lower close to nozzle compared to both 1/3rd and full-scale water models. This finding is consistent with the work of Creech [17]. Fig-7 and 5 show comparison of downward velocity at different vertical locations. Effect of shell moving downward with casting speed in caster and stationary wide & narrow faces of water model is clearly visible in downward velocity. Shell effect on flow diminished with downward distance from jet except close to narrow face (Fig-7). In, Fig-9 addition of shell showed similar trend in surface level as in velocity and is found giving slightly higher surface wave close to narrow face and a deeper dip in the central region.

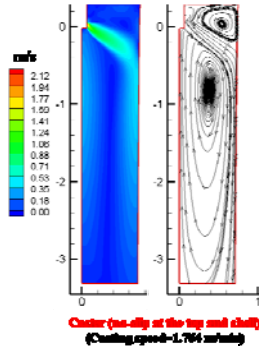

Fig-11 Velocity contours and streamlines in thick-slab steel caster with shell (Fr=0.005)

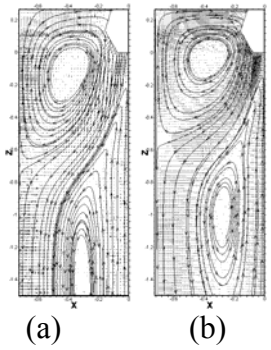

Fig-12 Velocity vector plots (with streamlines) along the wideface centerplane in thin-slab funnel mold and its full-scale water model for (a) 3.6 m/min Water Model, (b) 3.6 m/min Steel

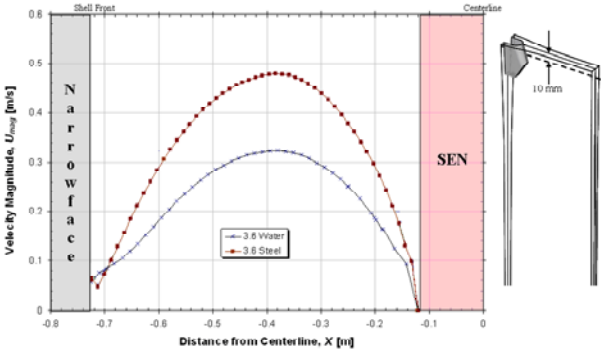

Fig-13 Velocity magnitude comparison along the wideface centerline in thin-slab funnel mold and its full-scale water model @ 10 mm below the top surface

Fig-12 shows velocity vectors and streamlines in thin-slab funnel mold and its full-scale water model. Both the water model and steel caster exhibit similar, characteristic double-roll flow patterns with the nozzle jet impinging on the narrow face wall. The water model predicts a straighter jet trajectory as it passes through the domain, yielding a lower jet impingement location and elongated rolls (in the z-direction) over the steel model. Lower recirculation zone is extended more towards outlet in water model than in corresponding steel caster. Fig-13 gives velocity magnitude plotted along the mid line between wide faces at 10 mm below free surface (along the dotted line in inset) in thin-slab funnel model and its full-scale water model. While both predict a maximum velocity at about 0.38 m from the center of the SEN, the fluid speed at this location is greatly underestimated by the water model (approximately 32% lower than the steel case, 0.324 m/s versus 0.478 m/s). The tapering of the shell and subsequent reduction in fluid cross-sectional area provides resistance for fluid leaving the domain. The higher resistance to downward flow in the steel case facilitates more fluid being "pushed" into the upper recirculation zone, yielding higher velocities at the top surface. As per expectations, the effect of shell at free surface velocity is more pronounced in thin-slab funnel mold compared to thick-slab mold. Same has to be confirmed in the lower region of the mold and yet to come next. Fig-14 and 15 shows the comparison of downward velocity at 1 and 2 m below surface respectively. At

both locations, shell has less effect at the mold center and showing around same velocity profile in the two. Close to narrow face, flow is more homogenized and flat in caster due to shell.

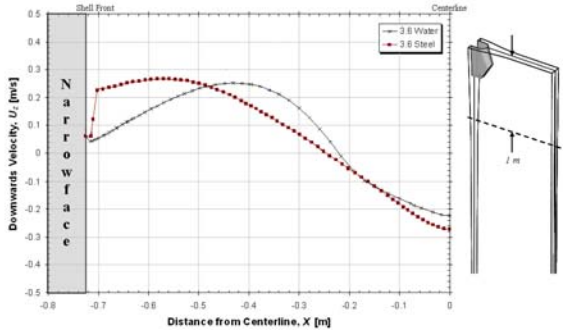

Fig-14 Downward velocity comparison along the wide face centerline in thin-slab funnel mold and its full-scale water model@ 1 m below the top surface

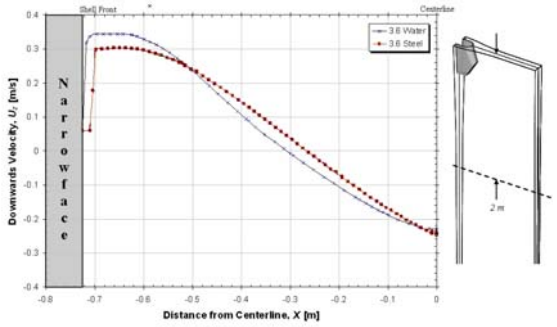

Fig-15 Downward velocity comparison along the wide face centerline in thin-slab funnel mold and its full-scale water model@ 2 m below the top surface

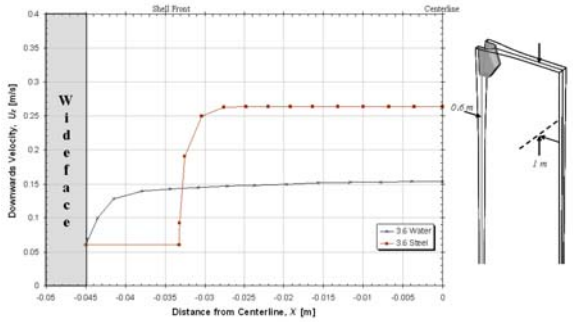

Fig-16 Downward velocity comparison @ 0.6 m from narrow face centerline in thin-slab funnel mold and its full-scale water model, 1 m below top surface

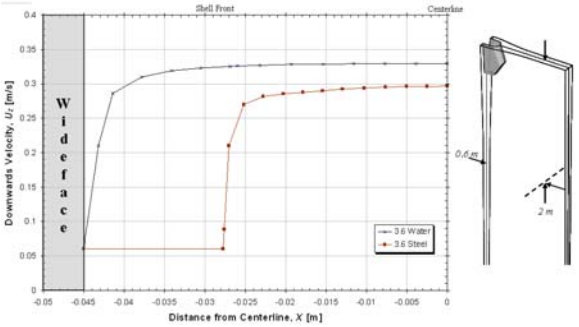

Fig-17 Downward velocity comparison in thin-slab funnel mold and its full-scale water model @ 0.6 m from narrow face centerline, 2 m below top surface

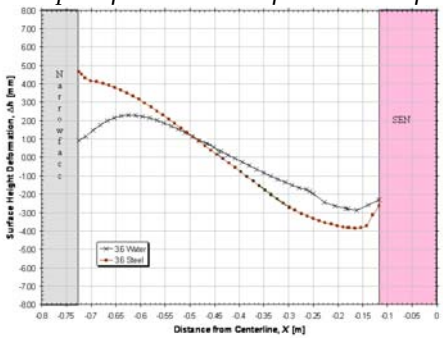

Fig-18 Top surface height approximation along wide face centerline in thin-slab funnel mold and its full-scale water model using fixed surface pressures

Fig-16 and 17 show downward velocity profiles for horizontal 2-D lines, parallel to and 0.6 m from the narrow face centerplane at 1 m and 2 m distances from the top surface respectively. The amount of liquid domain reduction due to solidification is easily seen in these figures. Since 1 m falls slightly above the jet hitting the narrow face and 2 m where jet straighten and falls with narrow face therefore as the distance from the top surface increases, the downward velocity for the water model progressively increases (relative to the steel plots). In the steel cases, solidification effects have a dissipative effect on flow in regard to velocity. It promotes more uniform flow patterns with velocities homogeneously approaching casting speeds as the distance to the top surface increases. Fig-18 gives free surface level along centerline between wide faces. In water model beads and in caster slag were used at the top for level calculations. The steel

caster shows around 5 times higher surface wave close to narrow face, level difference is not that significant close to nozzle again signifying reducing importance of shell in this region.

5.4. Other Effects

Effect of Mold Bottom:
Steel caster has no fixed bottom (the liquid pool tapers off with the steel solidification front until a solid slab is formed), the water model has a bottom plate which diverts fluid into recirculation channels. Though the presence of this unnatural bottom causes disruptions in fluid flow, its effect may be limited to the lower regions of the model [4]. Hypothetically it is possible to have a water model with a tall enough domain such that the effect of this bottom plate is nearly negligible at the top surface.
Thermal Buoyancy:
Temperature variation in the real caster may have significant effect on the flow patterns which is almost always missed by isothermal water models.
Effect of Multiphase Flow:
Apart from the presence of inclusions, argon gas is usually injected in the mold to avoid nozzle clogging and help inclusion removal therefore making the mold flow truly multiphase. Scaling of multiphase flow in addition to temperature variations in the mold is complicated and requires complex model formulations and even nearly impossible using water models.

6. Implications for Water Model Construction and Operation

- Qualitatively flow patterns are always okay in the top of the mold, sometimes get worse with distance down therefore be careful to interpret flow in lower recirculation zones since inaccuracies are caused by the bottom of water model, shell and perhaps even from thermal buoyancy.
- Full-scale water model is best, smaller scale is always ok in the top of the mold, but can deviate lower in strand if flow becomes laminar.

Surface velocity and free surface level can match steel caster if care is taken:

- Must have Froude similarity for a reduced scale water model to work, since gravitational forces are dominating.
- Best with a surface cover to slow down liquid, beads with density of ~400 kg/m^3 would be best (to match density ratio of slag to steel to capture free surface waves), but oil is okay too.
- Shell presence increases surface velocity (unavoidable), water model surface velocity is too low, owing to shell (thus, problem gets worse with decreasing slab thickness and decreasing casting speed).
- Putting the shell into water model makes the surface velocity too high (plastic does not move at casting speed). This error is even worse, so should not be done. (Evidence is given elsewhere [17]).
- Recognize that actual defect simulation (slag entrainment, etc.) will never match the steel caster. Must infer behavior by studying the surface velocity and level fluctuations. Look for keeping the time-average velocities in good ranges (windows of acceptable operation)

and to avoid occasional bad transients, jumps, glitching in flow (such as reported by Honeyands [5] and Chaudhary [14]).

7. Conclusions

In this work, effects of the water model scaling, free-surface condition and shell solidification have been analyzed using 1/3rd-, full-scale water models of thick-slab caster and full-scale water model of thin-slab funnel mold. For single-phase flow, satisfying Reynolds-Froude similarity requires full scale water model, downscaled water model with only Froude similarity matches flow patterns and surface waves with caster as long as flow regime (i.e. turbulent) is maintained same in both. Water models opened to atmosphere shows unreasonable high velocity and level variations therefore using beads or oil on the top having high enough viscosity imitating near no-slip boundary condition as in slag-steel case and same density ratio captures slag-steel interface features nicely. Effect of shell is minor in thick-slab caster but becomes much more significant in thin-slab funnel mold as shell thickness covers higher fraction of mold thickness than thick-slab mold.

Acknowledgments

Authors would like to acknowledge Continuous Casting Consortium, University of Illinois at Urbana-Champaign, IL, US and its members for supporting this project.

References

[1] Szekely J. and Yadoya R. T., *Metallurgical Transactions*, Vol. 3, Oct 1972, pp. 2673-2680.
[2] B.G. Thomas et al, *MCWASP IX*, Aachen, Germany, 2000, pp. 769-776.
[3] D. Gupta, and A.K. Lahiri, *Steel Research*, Vol. 63, No. 5, 1992, pp. 201-204.
[4] D. Gupta, S. Chakraborty, and A.K. Lahiri, *ISIJ Int.*, Vol. 37, No. 7, 1997, pp. 654-658.
[5] T. Honeyands and J. Herbertson, *Steel Research*, 1995. 66(7): p. 287-293.
[6] N. J. Lawson and M. R. Davidson, *J. of Fluids Eng-Trans of Asme*, 2002. 124(2): p. 535-543.
[7] S. Sivaramakrishnan, B. G. Thomas, and S. P. Vanka, *Mat Processing in the Computer Age*, V. Voller and H. Henein, Editors. 2000, TMS, Warrendale, PA. p. 189-198.
[8] Q. Yuan et al, *Met. & Mats Trans. B*, Vol. 35B, Oct 2004, pp. 967-982.
[9] Theodorakakos et al, *Met. & Mats Trans.B*,Vol.29B, Dec 1998, pp. 1321-1327.
[10] Ramos-banderas A. et al, *Met. & Materials Trans.B*,Vol.35B, Jun 2004, pp. 449-460.
[11] Li B. And Tsukihashi F., *ISIJ Int*, Vol. 45 (2005), No. 1, pp. 30-36.
[12] L. Zhang et al, *Met. & Mats Trans. B*, Vol. 38B, Feb 2007, pp. 63-83.
[13] Gupta D. and Lahari A. K., *Met. & Mats Trans. B*, Vol. 27B, Aug 1996, pp. 695-697.
[14] R. Chaudhary et al, *Mets & Mats Trans. B*, Vol. 39, No-6, Dec 2008.
[15]Y. A. Meng and B.G. Thomas, *Mets & Mats Trans* B, 2003. **34**(5): p. 685-705.
[16] G.A. Panaras et al, *Mets & Mats Trans*,Vol. 29B, No. 5, 1998, pp. 1112-1126.
[17] D. Creech, M.S. Thesis, University of Illinois at Urbana-Champaign, Urbana, 1999.